



Module 5E - Disease Contamination

Omar Betancourt, Payton Goodrich, Emre Mengi

June 23, 2023

BETA DRAFT

Contents

1	Theory	3
1.1	Introduction	3
1.2	Computational approaches for more complex models	4
1.2.1	More detailed characterization of the drag	4
2	Example	6
2.1	Simulation parameters	6
2.1.1	Particle generation	6
2.1.2	Initial trajectories	6
2.1.3	Numerical results	10
3	Assignment	11
4	Solution	15
5	Ethical Considerations for this Project	18
6	References	19

Objectives: Develop a model of how disease spreads through fine particles suspended in airborn droplets that are expelled from an infected individual when they cough.

Prerequisite Knowledge: High-school biology

Prerequisite Modules: 1A - Calculus, 1D - Differential Equations, 2C - Particle Dynamics, 3C - Generic Time Stepping

Difficulty: Hard

Summary:

The pandemic of 2020 has led to a huge interest of modeling and simulation of infectious diseases. One of the central questions is the potential infection zone produced by a cough. In this work, mathematical models are developed to simulate the progressive time-evolution of the distribution of locations of particles produced by a cough. Analytical and numerical studies are undertaken. The models ascertain the range, distribution and settling time of the particles under the influence of gravity and drag from the surrounding air. Beyond qualitative trends that illustrate that large particles travel far and settle quickly, while small particles do not travel far and settle slowly, the models provide quantitative results for distances travelled and settling times, which are needed for constructing social distancing policies and workplace protocols.

1 Theory

1.1 Introduction

The pandemic of 2020, due to SARS-CoV-2, named COVID-19 and referred to as coronavirus, has been responsible for hundreds of thousands of deaths in 2020 alone. It is well-established that this virus primarily spreads from person-to-person contact by respiratory droplets produced when an infected person coughs or sneezes. Subsequently, the droplets come into contact with the eyes, nose or mouth of a nearby person or when a person touches an infected surface, then makes contact with their eyes, nose or mouth. Since the virus is small, 0.06-0.14 microns in diameter, it can be contained in or attached to such emitted droplets. Droplets as small as one micron can carry enough viral load to cause an infection. A particular concern is the interaction of droplets with ventilation systems, which potentially could enhance the propagation of pathogens. This has implications on situation-specific safe distancing and the design of building filtration systems, air distribution, heating, air-conditioning and decontamination systems, for example using UV-c and related technologies. In order to facilitate such system redesigns, fundamental analysis tools are needed that are easy to use. Accordingly, this work develops one type of such needed tools, namely a simulator for the analysis of cough particle tracking, in order to ascertain how large is the potential infection zone and the airborne setting time of cough particles.

In its most basic form, a cough can be considered as a high-velocity release of a random distribution of particles of various sizes, into an ambient atmosphere. We refer the reader to Wei and Li [54], Duguid [12], Papineni and Rosenthal [38], Wei and Li [55], Zhu et al [59], Chao et al [9], Morawska et al [32], VanSciver et al [50], Kwon et al [21], Tang et al [26], Xie et al [48], Gupta et al [13], Wan et al [53], Villafruela et al. [51], Nielson [34] Zhang and Li [58] and Lindsley et. al [27] for extensive reviews of coughs and other respiratory emissions. Following formulations for physically similar problems associated with particulate dynamics from the fields of blasts, explosions and fire embers (Zohdi [64 ,65, 66, 67]), we make the following assumptions:

- We assume the same initial velocity magnitude for all particles under consideration, with a random distribution of outward directions away from the source of the cough. This implies that a particle non-interaction approximation is appropriate. Thus, the inter-particle collisions are negligible. This has been repeatedly verified by “brute-force” collision calculations using formulations found in Zohdi [60, 61, 62, 63].
- We assume that the particles are spherical with a random distribution of radii R_i , $i = 1, 2, 3...N = \text{particles}$. The masses are given by $m_i = \rho_i \frac{4}{3}\pi R_i^3$, where ρ_i is the density of the particles.

- We assume that the cough particles are *quite small* and that the amount of rotation, if any, contributes negligibly to the overall trajectory of the particles. The equation of motion for the i^{th} particle in the system is

$$m_i \dot{\mathbf{v}}_i = \Psi_i^{grav} + \Psi_i^{drag}, \quad (1.1)$$

with initial velocity $\mathbf{v}_i(0)$ and initial position $\mathbf{r}_i(0)$. The gravitational force is $\Psi_i^{grav} = m_i \mathbf{g}$, where $\mathbf{g} = (g_x, g_y, g_z) = (0, 0, -9.81) \text{ m/s}^2$.

- For the drag, we will employ a general phenomenological model

$$\Psi_i^{drag} = \frac{1}{2} \rho_a C_D \|\mathbf{v}^f - \mathbf{v}_i\| (\mathbf{v}^f - \mathbf{v}_i) A_i, \quad (1.2)$$

where C_D is the drag coefficient, A_i is the reference area, which for a sphere is $A_i = \pi R_i^2$, ρ_a is the density of the ambient fluid environment and \mathbf{v}^f is the velocity of the surrounding medium which, in the case of interest, is air. We will assume that the velocity of the surrounding fluid medium (\mathbf{v}^f) is given, implicitly assuming that the dynamics of the surrounding medium are unaffected by the particles.¹

In order to gain insight, initially, reader may refer back to the Particle Kinematics module on the closely related, analytically tractable, Stokesian Model.

Remarks: As mentioned, there are a large number of physically similar phenomena to a cough, such as the particulate dynamics associated with blasts, explosions and fire embers. We refer the interested reader to the wide array of literature on this topic; see Plimpton [40], Brock [6], Russell [41], Shimanzu [42], Werrett [56], Kazuma [19, 20], Wingerden et al [57] and Fernandez-Pello [10], Pleasance and Hart [39], Stokes [46] and Rowntree and Stokes [44], Hadden et al [14], Urban et al [49] and Zohdi [67].

1.2 Computational approaches for more complex models

1.2.1 More detailed characterization of the drag

In order to more accurately model the effects of drag, one can take into account that the empirical drag coefficient varies with Reynolds number. For example, consider the following piecewise relation (Chow [9]):

- For $0 < Re \leq 1$, $C_D = \frac{24}{Re}$,
- For $1 < Re \leq 400$, $C_D = \frac{24}{Re^{0.646}}$,
- For $400 < Re \leq 3 \times 10^5$, $C_D = 0.5$,
- For $3 \times 10^5 < Re \leq 2 \times 10^6$, $C_D = 0.000366 Re^{0.4275}$ and
- For $2 \times 10^6 < Re < \infty$, $C_D = 0.18$,

where, as in the previous section, the local Reynolds number for a particle is $Re \stackrel{\text{def}}{=} \frac{2R_i \rho_a \|\mathbf{v}^f - \mathbf{v}_i\|}{\mu_f}$ and μ_f is the fluid viscosity.² We note that in the zero Reynolds number limit, the drag is Stokesian. In order to solve the governing equation,

$$m_i \dot{\mathbf{v}}_i = \Psi_i^{grav} + \Psi_i^{drag} = m_i \mathbf{g} + \frac{1}{2} \rho_a C_D \|\mathbf{v}^f - \mathbf{v}_i\| (\mathbf{v}^f - \mathbf{v}_i) A_i, \quad (1.3)$$

we integrate the velocity numerically

$$\mathbf{v}_i(t + \Delta t) = \mathbf{v}_i(t) + \frac{1}{m_i} \int_t^{t+\Delta t} (\Psi_i^{grav} + \Psi_i^{drag}) dt \approx \mathbf{v}_i(t) + \frac{\Delta t}{m_i} (\Psi_i^{grav}(t) + \Psi_i^{drag}(t)). \quad (1.4)$$

¹We will discuss these assumptions further, later in the work.

²The viscosity coefficient for air is $\mu_f = 0.000018 \text{ Pa}\cdot\text{s}$.

The position is obtained by integrating again:

$$\mathbf{r}_i(t + \Delta t) = \mathbf{r}_i(t) + \int_t^{t+\Delta t} \mathbf{v}_i(t) dt \approx \mathbf{r}_i(t) + \Delta t \mathbf{v}_i(t). \quad (1.5)$$

This approach has been used repeatedly for a variety of physically similar drift-type problems in Zohdi [64, 65, 66, 67].

Remark: The piecewise drag law of Chow [9] is a mathematical description for the Reynolds number over a wide range and is a curve-fit of extensive data from Schlichting [45].

2 Example

2.1 Simulation parameters

In order to illustrate the model, the following simulation parameters were chosen:

- Starting height of 2 meters,
- Total simulation duration, 4 seconds,
- The time step size, $\Delta t = 10^{-6}$ seconds,
- The cough velocity, $V^c(t = 0) = 30 \text{ m/s}$ (taken from the literature which indicates $10 \text{ m/s} \leq V^c \leq 50 \text{ m/s}$),
- Density of particles, $\rho_i = 1000, \text{ kg/m}^3$,
- Density of air, $\rho_a = 1.225, \text{ kg/m}^3$ and
- Total mass, $M^{Total} = \sum_{i=1}^{P_n} m_i = 0.0005 \text{ kg}$.

2.1.1 Particle generation

A mean particle radius was chosen to be $\bar{R} = 0.0001 \text{ m}$ with variations according to

$$R_i = \bar{R} \times (1 + A \times \zeta_i), \quad (2.1)$$

where $A = 0.9975$ and a random variable $-1 \leq \zeta_i \leq 1$. The algorithm used for particle generation was:

- M=0
- Start loop: $i = 1, P_n$
- $R_i = \bar{R} \times (1 + A \times \zeta_i)$,
- $M = M + m_i = M + \rho_i \frac{4}{3} \pi R_i^3$
- If $M \geq M^{Total}$ then stop (determines $P_n = \text{particles}$)
- End loop

2.1.2 Initial trajectories

The initial trajectories we determined from the following algorithm

- Specify relative direction 'cone' parameters: $\mathbf{N}^c = (N_x^c, N_y^c, N_z^c)$,
- For each particle, $i = 1, 2, 3, \dots, P_n$, construct a (perturbed) trajectory vector:

$$\mathbf{N}_i = (N_x^c + A_x^c \times \eta_{ix}, N_y^c + A_y^c \times \eta_{iy}, N_z^c + A_z^c \times \eta_{iz}) = (N_{ix}, N_{iy}, N_{iz}), \quad (2.2)$$

where $-1 \leq \eta_{ix} \leq 1$, $0 \leq \eta_{iy} \leq 1$ and $-1 \leq \eta_{iz} \leq 1$.

- For each particle, normalize the trajectory vector:

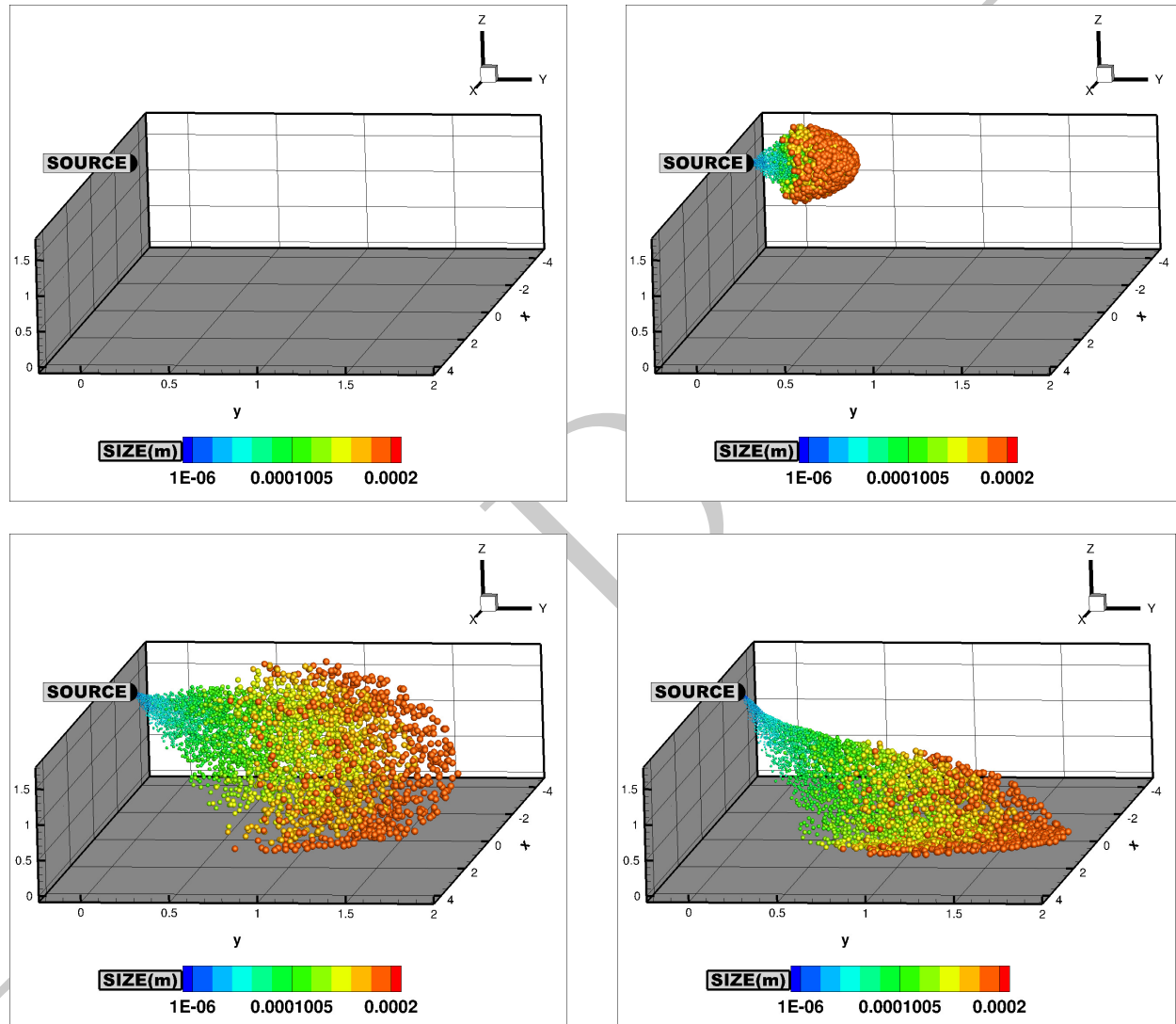
$$\mathbf{N}_i = \frac{1}{\|\mathbf{N}_i\|} (N_{ix}, N_{iy}, N_{iz}). \quad (2.3)$$

- For each particle, the velocity vector is constructed by a projection onto the normal vector:

$$\mathbf{v}_i = V^c \mathbf{N}_i. \quad (2.4)$$

$v_y^f(m/s)$	Max - distance(m)	Comments
-2.0	8.002	due to small particles moving backwards
-1.0	4.210	due to small particles moving backwards
0.0	2.721	due to large particles moving forwards
1.0	4.937	due to large particles moving forwards
2.0	8.736	due to large particles moving forwards

Table 2.1: Maximum distance from the source at the end of T=4 seconds.



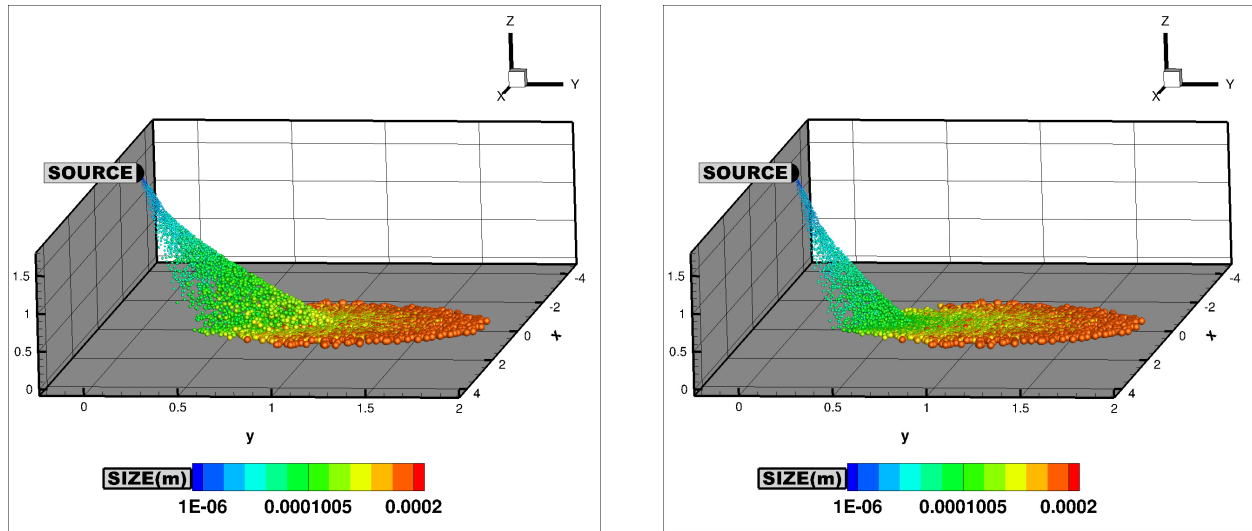
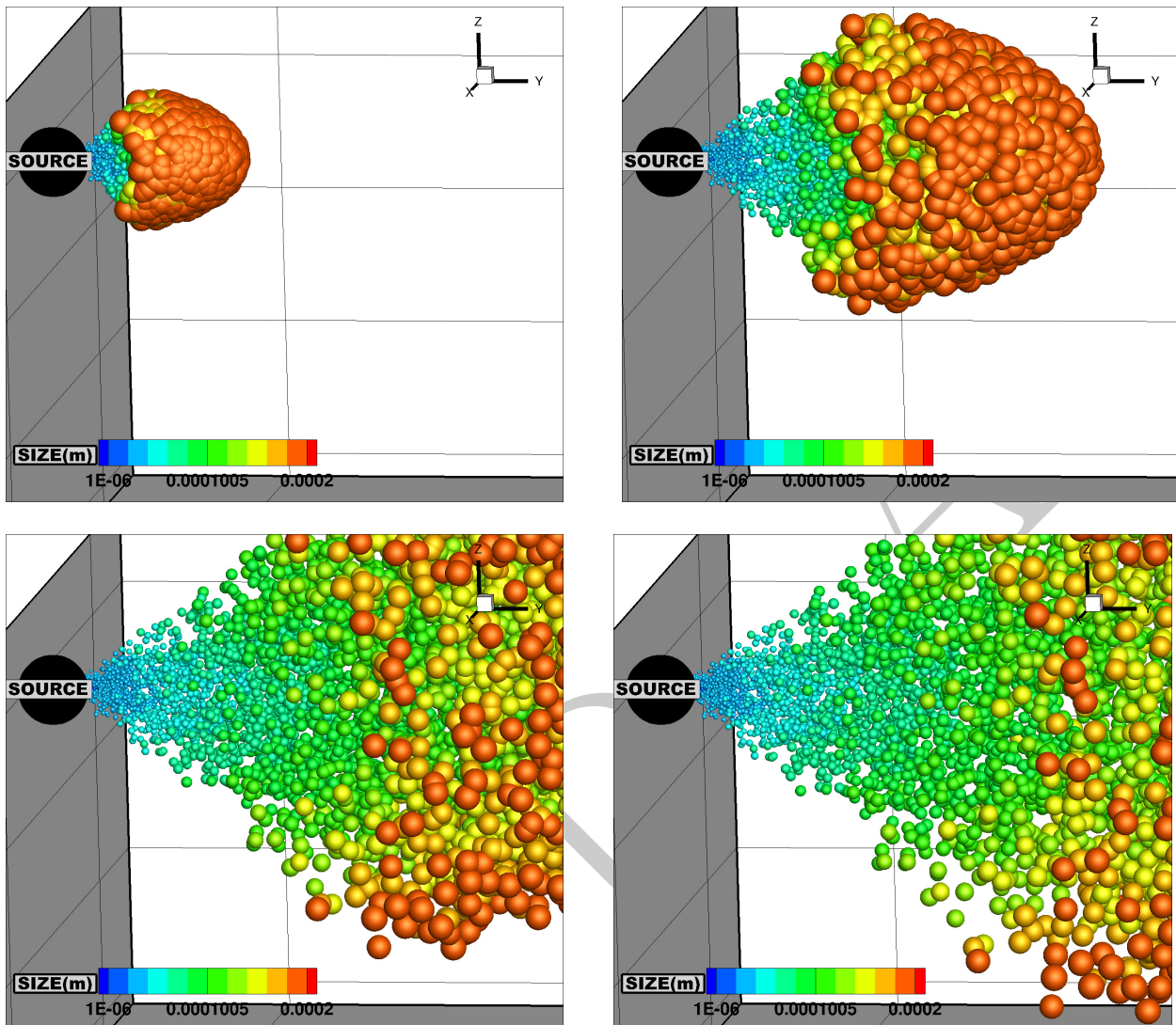


Figure 2.2: Cough simulation (from a starting height of 2 meters, for $v^f = (0, 0, 0)$): successive frames indicating the spread of particles. (a) Large particles travel far and settle quickly and (b) Small particles do not travel far and settle slowly.



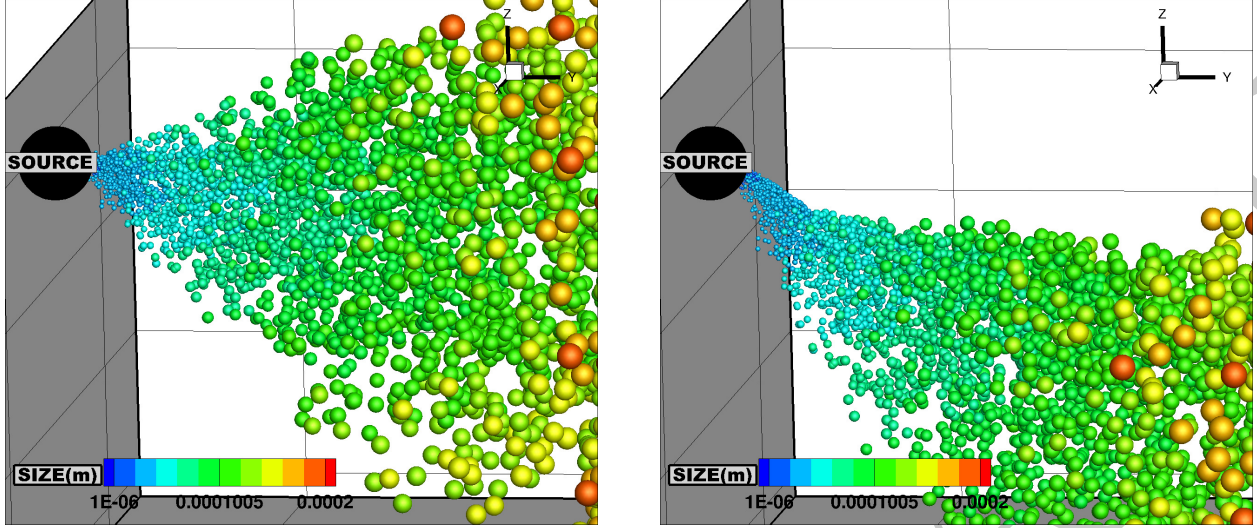


Figure 2.4: Zoom on cough simulation (from a starting height of 2 meters, for $\mathbf{v}^f = (0, 0, 0)$): successive frames indicating the spread of particles. (a) Large particles travel far and settle quickly and (b) Small particles do not travel far and settle slowly.

2.1.3 Numerical results

An extremely small (relative to the total simulation time) time-step size of $\Delta t = 10^{-6}$ seconds was used. Further reductions of the time-step size produced no noticeable changes in the results, thus the solutions generated can be considered to have negligible numerical error. The simulations took under 10 seconds on a standard laptop. The algorithm generated 59941 particles ranging from $2.5 \times 10^{-7} m \leq R_i \leq 2 \times 10^{-4} m$ (i.e. $0.25 \text{ microns} \leq R_i \leq 200 \text{ microns}$). We used a trajectory cone of $\mathbf{N}^c = (0, 1, 0)$ and $\mathbf{A}^c = (1, 0.5, 1)$ in the example given. Figures 2.2-2.4 illustrate the results for the parameters above (for $v_y^f = 0$). If particles contacted the floor, they were immobilized. The maximum distance travelled from the source located at $(0, 0, 2)$ was 2.72 meters (achieved by large particles). Table 2.1 shows variation in the headwind. For strong tailwind, the larger particles land further away from the cough source. As the analytical theory asserts, successive frames indicate that: (a) Large particles travel far and settle quickly and (b) Small particles do not travel far and settle slowly (when there are no ambient velocities). As observed in the simulations, the settling of the small particles is still not achieved by the end of the simulation time (here 4 seconds). Accordingly, the simulations were also run for extremely long periods to ascertain that the "mist" of small particles remained airborne for several minutes (as predicted by the theory). For strong opposing headwind, small particles move backwards, and still remain airborne for extended periods of time. *This is by far the most dangerous case, since this will encounter other persons at the torso level.* We also note that ratio of the general drag to gravity indicates:

$$\frac{\|\Psi^{drag,general}\|}{\|\Psi^{grav}\|} = \frac{3C_D\rho_a\|\mathbf{v}^f - \mathbf{v}_i\|^2}{\rho_i R_i g}, \quad (2.5)$$

which indicates that at high velocities, the dynamics are dominated by drag.

3 Assignment

The pandemic of 2020 has led to a huge interest of modeling and simulation of infectious diseases. One of the central questions is the potential infection zone produced by a cough. In this assignment, you will develop mathematical models to simulate the progressive time-evolution of the distribution of particles in space produced by a cough. You will be asked that you recommend safe distancing guidelines based on the range, distribution and settling time of the particles under the influence of gravity and drag from the surrounding air.

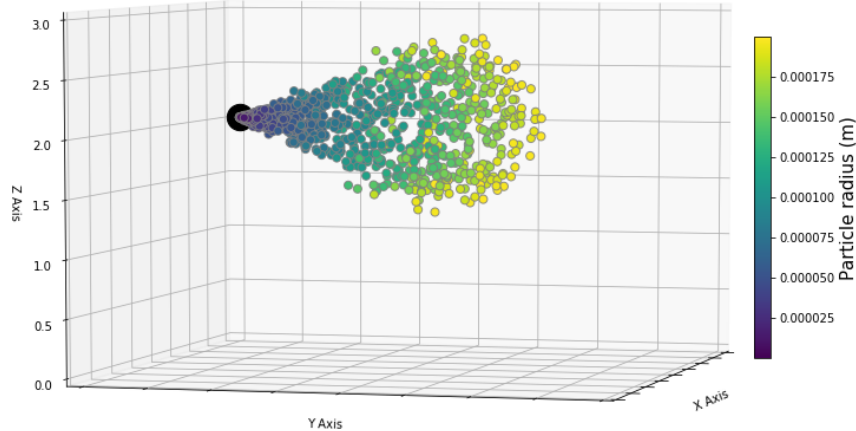


Figure 3.1: Droplet dispersion after 0.1 seconds.

The template code to complete the project is given here on [GitHub](#).

Problem 1: Theory-Based Exercises

Answer the following questions *prior* to coding the assignment to better understand the background physics and mathematics that govern the given models. You **may** solve these problems by hand **and/or** using computational tools such as Python etc. Please include all handwritten work and code used to solve each problem.

Problem 1.1

Given the particles are spherical with a random distribution of radii $R_i, i = 1, 2, 3, \dots, N = \text{particles}$ and the masses are given by $m_i = \rho_i \frac{4}{3}\pi R_i^3$, where ρ_i is the density of the particles and is assumed to be constant for all droplets, the equation of motion for the i th particle in the system is

$$m_i \ddot{\mathbf{r}}_i = \Psi_i^{grav} + \Psi_i^{drag} \quad (3.1)$$

where m_i is the mass of each droplet, $\ddot{\mathbf{r}}_i$ is the droplet's acceleration, and the two Ψ are gravitational and drag forces respectively.

Let the z axis be the vertical axis so we note that the gravitation force be defined as

$$\Psi_i^{grav} = m_i(g_x, g_y, g_z) = (0, 0, -m_i g) \quad (3.2)$$

where g is the gravitational constant. The drag force depends on the geometry of the droplet and the properties of the surrounding medium:

$$\Psi_i^{drag} = \frac{1}{2} \rho_a C_D ||\mathbf{v}^f - \mathbf{v}_i|| (\mathbf{v}^f - \mathbf{v}_i) A_i \quad (3.3)$$

where C_D is the drag coefficient, A_i is the reference area, which for a sphere is $A_i = \pi R_i^2$, ρ_a is the density of the ambient fluid environment and \mathbf{v}^f is the velocity of the surrounding medium, which in this case is air.

Solve for the acceleration of the particle and plug in the individual equations for Ψ_i^{grav} , Ψ_i^{drag} , and m .

Problem 1.2

To determine the drag coefficient, we first determine the Reynolds number of the droplet Re :

$$Re = \frac{2R\rho_a \|\mathbf{v}^f - \mathbf{v}_i\|}{\mu_f} \quad (3.4)$$

Where μ_f is the viscosity of the surrounding medium. Then, the drag coefficient is a piecewise function of Re :

$$C_{Di} = \begin{cases} \frac{24}{Re}, & 0 < Re \leq 1 \\ \frac{24}{Re^{0.646}}, & 1 < Re \leq 400 \\ 0.5, & 400 < Re \leq 3 \times 10^5 \\ 0.000366Re^{0.4275}, & 3 \times 10^5 < Re \leq 2 \times 10^6 \\ 0.18, & Re > 2 \times 10^6 \end{cases} \quad (3.5)$$

Given the variable glossary values, write the piece-wise drag coefficient in terms of particle velocity.

Problem 1.3

We have the governing equation for the motion of the droplets, which we will numerically integrate using the Forward Euler method. Write down the Forward Euler scheme to integrate and find the position and velocity of some i -th droplet.

Problem 2: Coding Exercises

Use the given python notebook template to complete the following coding exercises.

Problem 2.1

Define the constants used in the simulation. Use the variable glossary at the end of the assignment.

Problem 2.2

Let us assume the total mass of all of the droplets in a cough is $M^{total} = 0.00005kg$, with a mean particle radius of $\bar{R} = 0.0001m$ with variations according to

$$R_i = \bar{R} \times (1 + A \times \xi_i) \quad (3.6)$$

where $A = 0.9975$ and a random variable $-1 \leq \xi_i \leq 1$. The algorithm used for particle generation should be:

- Initialize total mass: $M = 0$
- Start loop: $i = 1, P_n$
- Compute a random deviation from the mean radius \bar{R} : $R_i = \bar{R} \times (1 + A \times \xi_i)$
- Compute the mass of the new particle and add to the total mass computed: $M = M + m_i = M + \rho_i \frac{4}{3} \pi R_i^3$

- Check if the threshold for total mass has been reached: If $M \geq M^{total}$ then stop (**determines $P_n = \text{particles}$**)
- End loop.

Initialize the particles size and mass randomly using the described algorithm.

Problem 2.3

The initial trajectories we determined from the following algorithm:

- Specify the relative direction of the cough: $\mathbf{N}^c = (N_x^c, N_y^c, N_z^c)$,
- For each particle, $i = 1, 2, 3, \dots, P_n$, construct a (perturbed) trajectory vector:

$$\mathbf{N}_i = (N_x^c + A_x^c \times \eta_{ix}, N_y^c + A_y^c \times \eta_{iy}, N_z^c + A_z^c \times \eta_{iz}), \quad (3.7)$$

where the random cone parameters are bounded: $-1 \leq \eta_{ix} \leq 1$, $0 \leq \eta_{iy} \leq 1$, $-1 \leq \eta_{iz} \leq 1$.

- For each particle, normalize the trajectory vector:

$$\mathbf{n}_i = \frac{1}{\|\mathbf{N}_i\|_2} (N_{ix}, N_{iy}, N_{iz}). \quad (3.8)$$

- For each particle, the velocity vector is constructed by a projection onto the normal vector:

$$\mathbf{v}_i = V^c \mathbf{n}_i \quad (3.9)$$

Initialize particle velocities using the described algorithm.

Problem 2.4

Run the simulator. The resulting video will be saved as 'animation.mp4' in the same directory as the notebook.

Problem 3: Analyzing Your Results

Answer the following questions about the code you created.

Problem 3.1

Report approximately how far the particles landed from the starting point. Does the simulation agree with the prescribed '6-feet' social distancing recommendation from authorities?

Problem 3.2

Knowing the particle size range used in the simulation, what percentage of the particles contaminating the air can be captured by a standard N95 mask?

VARIABLE GLOSSARY

Symbol	Type	Units	Value	Description
r_0	Vector	m	[0, 0, 2]	Standing height
t_{tot}	Scalar	s	4	Total simulation time
dt	Scalar	s	1e-4	Time step
$V_{t=0}^c$	Scalar	m/s	35	Cough velocity
V^f	Vector	m/s	[0, 0, 0]	Velocity of surrounding medium
ρ_i	Scalar	kg/m ³	1000	Density of droplets
ρ_a	Scalar	kg/m ³	1.225	Density of air
M^{total}	Scalar	kg	0.00005	Total mass $\sum_{i=1}^{P_n} m_i$
\bar{R}	Scalar	m	0.0001	Mean particle radius
A	Scalar	none	0.9975	Deviatoric constant
\mathbf{N}^c	vector	none	[0, 1, 0]	Trajectory cone
\mathbf{A}^c	vector	none	[1, 0.5, 1]	Deviatoric constant for trajectory
μ_f	scalar	Pa · s	1.8e-5	Viscosity coefficient for air
g	vector	m/s ²	[0, 0, -9.81]	Gravitational constant

4 Solution

Problem 1: Theory-Based Exercises

Problem 1.1

Solve for the acceleration of the particle and plug in the individual equations for Ψ_i^{grav} , Ψ_i^{drag} , and m .
Given

$$\Psi_i^{grav} = m_i(g_x, g_y, g_z) = (0, 0, -m_i g) \quad (4.1)$$

$$\Psi_i^{drag} = \frac{1}{2}\rho_a C_D \|\mathbf{v}^f - \mathbf{v}_i\| (\mathbf{v}^f - \mathbf{v}_i) A_i \quad (4.2)$$

$$m_i \ddot{\mathbf{r}}_i = \Psi_i^{grav} + \Psi_i^{drag} \quad (4.3)$$

$$m_i = \rho_i \frac{4}{3} \pi R_i^3 \quad (4.4)$$

Then,

$$\ddot{\mathbf{r}}_i = \frac{1}{\rho_i \frac{4}{3} \pi R_i^3} \left(m_i \mathbf{g} + \frac{1}{2} \rho_a C_D \|\mathbf{v}^f - \mathbf{v}_i\| (\mathbf{v}^f - \mathbf{v}_i) A_i \right) \quad (4.5)$$

Problem 1.2

Given the variable glossary values, write the piece-wise drag coefficient in terms of particle velocity.

Given:

$$Re = \frac{2R\rho_a \|\mathbf{v}^f - \mathbf{v}_i\|}{\mu_f} \quad (4.6)$$

$$Re = \frac{2(0.0001)(1.225)\|\mathbf{v}_i\|}{1.8e-5} \quad (4.7)$$

$$Re = 13.61 \|\mathbf{v}_i\| \quad (4.8)$$

$$C_{Di} = \begin{cases} \frac{24}{13.61 \|\mathbf{v}_i\|}, & 0 < 13.61 \|\mathbf{v}_i\| \leq 1 \\ \frac{24}{(13.61 \|\mathbf{v}_i\|)^{0.646}}, & 1 < 13.61 \|\mathbf{v}_i\| \leq 400 \\ 0.5, & 400 < 13.61 \|\mathbf{v}_i\| \leq 3 \times 10^5 \\ 0.000366(13.61 \|\mathbf{v}_i\|)^{0.4275}, & 3 \times 10^5 < 13.61 \|\mathbf{v}_i\| \leq 2 \times 10^6 \\ 0.18, & 13.61 \|\mathbf{v}_i\| > 2 \times 10^6 \end{cases} \quad (4.9)$$

Problem 1.3

Write down the Forward Euler scheme to integrate and find the position and velocity of some i -th droplet:

$$\mathbf{r}_i(t + \Delta t) = \mathbf{r}_i(t) + \Delta t \mathbf{v}_i(t) \quad (4.10)$$

$$\mathbf{v}_i(t + \Delta t) = \mathbf{v}_i(t) + \frac{\Delta t}{m_i} \Psi_i^{grav}(t) \quad (4.11)$$

Problem 2: Coding Exercises

Use the given python notebook template to complete the following coding exercises.

Problem 2.1

Define the constants used in the simulation. Use the variable glossary at the end of the assignment.

Solution Cell Block:

```

1 # ##### Problem 2.1 #####
2 ##### #####
3
4 #----- constants -----
5 r0 = np.array([0, 0, 2]).T      # starting height (m) #FILL IN HERE
6 g = np.array([0, 0, -9.81]).T   # gravity (m/s^2) #FILL IN HERE
7
8 t_tot = 4                      # simulation time (s) #FILL IN HERE
9 dt = 1e-4                       # time step (s) #FILL IN HERE
10 V0 = 30                         # magnitude of cough velocity (m / s) #FILL IN HERE
11 rho = 1000                      # density of particles (kg / m^3) #FILL IN HERE
12 mTot = 0.00005                  # total mass of droplets (kg) #FILL IN HERE
13
14 vf = np.array([0, 0, 0]).T       # surrounding fluid velocity (m/s) #FILL IN HERE
15 muf = 1.8e-5                   # surrounding fluid viscosity (Pa/s) #FILL IN HERE
16 rhoF = 1.225                    # density of air (kg / m^3) #FILL IN HERE

```

Problem 2.2

Initialize the particles size and mass randomly using the described algorithm.

Problem 2.3

Initialize particle velocities using the described algorithm.

Problem 2.4

Run the simulator. The resulting video will be saved as 'animation.mp4' in the same directory as the notebook.

Problem 3: Analyzing Your Results

Answer the following questions about the code you created.

Problem 3.1

Report approximately how far the particles landed from the starting point. Does the simulation agree with the prescribed '6-feet' social distancing recommendation from authorities?

The particles landed approximately 1.5 meters from the starting point. This is around 5 feet, which is close to the 6 feet social distancing recommendation. However, any air currents or wind could have affected the particles' trajectories, so the particles could have landed further away from the starting point. In addition, we see that the smaller particles remained in the air for a longer time, which would be dangerous for any person moving through the cloud of particles at a later time.

Problem 3.2

Knowing the particle size range used in the simulation, what percentage of the particles contaminating the air can be captured by a standard N95 mask?

The average size of the particles is 0.0001 meters. The N95 mask can filter out particles that are 0.3 microns or larger. This means that the N95 mask can filter out 99.9% of the particles in the simulation. This proves that wearing a mask is an effective way to prevent the spread of COVID-19.

BETA DRAFT

5 Ethical Considerations for this Project

A goal of this project is to enable advancements in science and engineering through to address critical national challenges associated with next generation food systems. There are deep ethical considerations associated with any technology, in particular for food systems. While technology has tremendous potential to identify greater efficiencies, when it is created without appropriate consideration for who will have access to and control over new resources, or how the new technologies will impact those who work in the system, the efficiencies identified may come at the cost of greater societal inequity. It is important to pursue harnessing technology to disrupt existing inequities, rather than further entrench existing power structures. The following areas should be considered:

- Labor: 1) occupational health, 2) food manufacturing, and 3) outdoor agriculture labor;
- Producers: 1) Small- to mid-size farms, 2) urban agriculture, and 3) research in farm transitions;
- Technology: 1) research in technology and democracy;
- Health Human Rights: 1) land rights, 2) social justice, and 3) decolonization in agriculture;

Please consider the following questions:

- What are the societal implications of the technology that you are developing?
- Can this technology be distributed fairly and equitably to a wide variety of entities in agricultural industry?
- Are there any potential unintended consequences of this technology becoming available?
- Are there any harmful “spinoffs” of this technology?
- Are there any useful “spinoffs” of this technology?

6 References

1. Anderson, J. G., Rowan, N. J., MacGregor, S. J., Fouracre, R. A., & Farish, O. (2000). Inactivation of food-borne enteropathogenic bacteria and spoilage fungi using pulsed-light. IEEE Transactions on Plasma Science , 28 (1), 83-88.
2. Avci, B. and Wriggers, P. (2012). A DEM-FEM coupling approach for the direct numerical simulation of 3D particulate flows, Journal of Applied Mechanics, Vol. 79, 010901-(1-7).
3. Battelle (2020). Instructions for Healthcare Personnel: Preparation of Compatible N95 Respirators for Decontamination by the Battelle Memorial Institute Using the Battelle Decontamination System. <https://www.fda.gov/media/137032/download>
4. Bolintineanu, D. S., Grest, G. S., Lechman, J. B., Pierce, F., Plimpton, S. J. and Schunk, P. R (2014). Particle dynamics modeling methods for colloid suspensions. Computational Particle Mechanics, Volume 1, Issue 3, pp 321-356.
5. Boyce, JM (2016). "Modern technologies for improving cleaning and disinfection of environmental surfaces in hospitals". Antimicrobial Resistance and Infection Control. 5: 10. doi:10.1186/s13756-016-0111-x. PMC 4827199. PMID 27069623.
6. Brock, A. St. Hill (1949). A History of Fireworks. George G. Harrap and Co.
7. Card, K. J., Crozier, D., Dhawan, A., Dinh, M., Dolson, E., Farrokhan, N., Gopalakrishnan, V., Ho, E., King, E. S., Krishnan, N., Kuzmin, G., Maltas, J., Pelesko, J., Scarborough, J. A., Scott, J. G., Sedor, G., & Weaver, D. T. (2020). UV Sterilization of Personal Protective Equipment with Idle Laboratory Biosafety Cabinets During the Covid-19 Pandemic [Preprint]. Occupational and Environmental Health. <https://doi.org/10.1101/2020.03.25.20043489>
8. Chao CYH, Wan MP, Morawska L, Johnson GR, Ristovski ZD, Hargreaves M, et al. Characterization of expiration air jets and droplet size distributions immediately at the mouth opening. Journal of Aerosol Science. 2009; 40 (2): 122-133.
9. Chow, C. Y. (1980). An introduction to computational fluid dynamics. New York, Wiley.
10. Fernandez-Pello, A. C. (2017). Wildland fire spot ignition by sparks and firebrands. Fire Safety Journal, 91 2-10.
11. Downes, A. and Blunt, T. P. (1878). On the Influence of Light upon Protoplasm. Proceedings of the Royal Society of London. 28 (190-195): 199-212. Bibcode:1878RSPS...28..199D. doi:10.1098/rspl.1878.0109
12. Duguid JP. The size and the duration of air-carriage of expiratory droplets and droplet-nuclei. Journal of Hygiene. 1946; 44: 471-479.
13. Gupta JK, Lin CH and Chen Q. Flow dynamics and characterization of a cough. Indoor Air. 2009; 19 (6): 517-525. pmid:19840145
14. Hadden, R., Scott, S., Lautenberger, C. and Fernandez-Pello, C. A.(2011). Ignition of combustible fuel beds by hot particles: an experimental and theoretical study, Fire Technol. 47 341-355.
15. Heimbuch, B. and Harnish, D. (2019). Research to Mitigate a Shortage of Respiratory Protection Devices During Public Health Emergencies (Report to the FDA No. HHSF223201400158C). Applied Research Associate, Inc.
16. Heimbuch, B. K., Wallace, W. H., Kinney, K., Lumley, A. E., Wu, C.-Y., Woo, M.-H., & Wander, J. D. (2011). A pandemic influenza preparedness study: Use of energetic methods to decontaminate filtering facepiece respirators contaminated with H1N1 aerosols and droplets. American Journal of Infection Control , 39 (1), e1-e9.
17. Ito, A., & Ito, T. (1986). Absorption spectra of deoxyribose, ribosephosphate, ATP and DNA by direct transmission measurements in the vacuum-UV (150-190 nm) and far-UV (190-260 nm) regions using synchrotron radiation as a light source. Photochemistry and Photobiology , 44 (3), 355-358.
18. Kanemitsu, K. et al, (2005) Does incineration turn infectious waste aseptic?, Journal of Hospital Infection, 60(4):304-306.

19. Kazuma, S. (2004). Hanabi no Hon. Fireworks Book . Tankosha. ISBN 4-473-03177-2.
20. Kazuma, S. (2011). Wonder of Fireworks. Soft Bank Creative. ISBN 978-4-7973-6450-7.
21. Kwon S-B, Park J, Jang J, Cho Y, Park D-S, Kim C, et al. Study on the initial velocity distribution of exhaled air from coughing and speaking. *Chemosphere*. 2012; 87 (11): 1260-1264. pmid:22342283
22. Labra, C. and Onate E. 2009. High-density sphere packing for discrete element method simulations. *Communications in Numerical Methods in Engineering*, Vol. 25 (7), pp. 837-849.
23. Leonardi, A., Wittel, F. K., Mendoza, M and Herrmann, H. J. (2014). Coupled DEM-LBM method for the free-surface simulation of heterogeneous suspensions. *Computational Particle Mechanics*, Volume 1, Issue 1, pp 3-13.
24. Lin, T.-H., Tang, F.-C., Hung, P.-C., Hua, Z.-C., & Lai, C.-Y. (2018). Relative survival of *Bacillus subtilis* spores loaded on filtering facepiece respirators after five decontamination methods. *Indoor Air* , 28 (5), 754-762.
25. Lindsley, W. G., Martin, S. B., Thewlis, R. E., Sarkisian, K., Nwoko, J. O., Mead, K. R., & Noti, J. D. (2015). Effects of Ultraviolet Germicidal Irradiation (UVGI) on N95 Respirator Filtration Performance and Structural Integrity. *Journal of Occupational and Environmental Hygiene* , 12 (8), 509-517. <https://doi.org/10.1080/15459624.2015.1018518>
26. Tang JW and Settles GS. Coughing and aerosols. *New England Journal of Medicine*. 2008; 359 (15): e19. pmid:18843121
27. William G. Lindsley, Terri A. Pearce, Judith B. Hudnall, Kristina A. Davis, Stephen M. Davis, Melanie A. Fisher, Rashida Khakoo, Jan E. Palmer, Karen E. Clark, Ismail Celik, Christopher C. Coffey, Francoise M. Blachere, and Donald H. Beezhold (2012) Quantity and Size Distribution of Cough-Generated Aerosol Particles Produced by Influenza Patients During and After Illness. *J Occup Environ Hyg*. 2012; 9(7): 443-449. Published online 2012 May 31. doi: 10.1080/15459624.2012.684582
28. Lore, M. B., Heimbuch, B. K., Brown, T. L., Wander, J. D., & Hinrichs, S. H. (2011). Effectiveness of Three Decontamination Treatments against Influenza Virus Applied to Filtering Facepiece Respirators. *The Annals of Occupational Hygiene* , 56 (1), 92-101.
29. Marra, A. R., Schweizer, M. L., & Edmond, M. B. (2018). No-Touch Disinfection Methods to Decrease Multidrug-Resistant Organism Infections: A Systematic Review and Meta-analysis. *Infection Control & Hospital Epidemiology* , 39 (1), 20-31.
30. Martin-Alberca, C. and Garcia-Ruiz, C. (2014). Analytical techniques for the analysis of consumer fireworks TrAC Trends in Analytical Chemistry, Volume 56, Pages 27-36.
31. Mills, D., Harnish, D. A., Lawrence, C., Sandoval-Powers, M., & Heimbuch, B. K. (2018). Ultraviolet germicidal irradiation of influenza-contaminated N95 filtering facepiece respirators. *American Journal of Infection Control* , 46 (7), e49-e55.
32. Morawska L, Johnson GR, Ristovski ZD, Hargreaves M, Mengersen K, Corbett S, et al. Size distribution and sites of origin of droplets expelled from the human respiratory tract during expiratory activities. *Journal of Aerosol Science*. 2009; 40(3): 256-269.
33. Nerandzic, M. M., Cadnum, J. L., Pultz, M. J., & Donskey, C. J. (2010). Evaluation of an automated ultraviolet radiation device for decontamination of *Clostridium difficile* and other healthcare-associated pathogens in hospital rooms. *BMC Infectious Diseases* , 10 (1), 197.
34. Nielsen PV. Control of airborne infectious diseases in ventilated spaces. *Journal of The Royal Society Interface*. 2009; 6(Suppl 6): S747-S755.
35. Onate, E., Idelsohn, S. R., Celigueta, M. A. and Rossi, R. (2008). Advances in the particle finite element method for the analysis of fluid-multibody interaction and bed erosion in free surface flows. *Computer Methods in Applied Mechanics and Engineering*, Vol. 197 (19-20), pp. 1777-1800.

36. Onate, E. and Celigueta, M. A. and Idelsohn, S. R. and Salazar, F. and Suárez, B. (2011). Possibilities of the Particle Finite Element Method for fluid-soil-structure interaction problems, Computational Mechanics, Vol. 48, 307-318.
37. Onate, E., Celigueta, M. A., Latorre, S., Casas, G., Rossi, R. and Rojek, J. (2014). Lagrangian analysis of multiscale particulate flows with the particle finite element method Computational Particle Mechanics, Volume 1, Issue 1, pp 85-102.
38. Papineni RS and Rosenthal FS. The size distribution of droplets in the exhaled breath of healthy human subjects. *Journal of Aerosol Medicine*. 1997; 10 (2): 105-116. pmid:10168531
39. Pleasance, G. E. and Hart, J. A (1977), An Examination of Particles from Conductors Clashing as Possible Source of Bushfire Ignition. State Electricity Commission of Victoria (SEC), Victoria, Australia, Research and Development Department, Report FM-1, 1977.
40. Plimpton, G. (1984). Fireworks: A History and Celebration. Doubleday. ISBN 0-385-15414-3.
41. Russell, M. S (2008). The chemistry of fireworks. Royal Society of Chemistry, Great Britain. ISBN 978-0-85404-127-5.
42. Shimizu, T. (1996). Fireworks: The Art, Science, and Technique. Pyrotechnica Publications. ISBN 978-0-929388-05-2.
43. Rojek J., Labra C., Su, O. and Onate, E. 2012. Comparative study of different discrete element models and evaluation of equivalent micromechanical parameters, International Journal of Solids and Structures, Vol 49, pp. 1497-1517, 2012 — DOI: 10.1016/j.ijsolstr.2012.02.032.
44. Rowntree, G. and Stokes, A. (1994), Fire ignition of aluminum particles of controlled size, *J. Electr. Electron. Eng.* (1994) 117-123.
45. Schlichtling, H. (1979). Boundary-layer theory. 7th edition. New York: McGraw-Hill.
46. Stokes, A. D., Fire ignition by copper particles of controlled size (1990) *J. Electr. Electron. Eng.*, Aust. 10, 188-194.
47. Tseng, C.-C., & Li, C.-S. (2007). Inactivation of Viruses on Surfaces by Ultraviolet Germicidal Irradiation. *Journal of Occupational and Environmental Hygiene* , 4 (6), 400-405.
48. Xie X, Li Y, Chwang ATY, Ho PL and Seto WH. How far droplets can move in indoor environments-revisiting the Wells evaporation-falling curve. *Indoor Air*. 2007; 17(3): 211-225. pmid:17542834
49. Urban, J. L., Zak, C. D., Song, J. and Fernandez-Pello, A. C., (2017). Smolder spot ignition of natural fuels by a hot metal particle, *Proc. Combust. Inst.* 36 (2) 3211-3218 ISSN 1540-7489 <https://doi.org/10.1016/j.proci.2016.09.014>.
50. VanSciver M, Miller S and Hertzberg J. Particle image velocimetry of human cough. *Aerosol Science and Technology*. 2011; 45 (3): 415-422.
51. Villafruela JM, Olmedo I, Ruiz De Adana M, Mendez C and Nielsen PV. CFD analysis of the human exhalation flow using different boundary conditions and ventilation strategies. *Building and Environment*. 2013; 62: 191-200.
52. Viscusi, D. J., Bergman, M. S., Eimer, B. C., & Shaffer, R. E. (2009). Evaluation of Five Decontamination Methods for Filtering Facepiece Respirators. *The Annals of Occupational Hygiene* , 53 (8), 815-827.
53. Wan MP, Sze To GN, Chao CYH, Fang L and Melikov A. Modeling the fate of expiratory aerosols and the associated infection risk in an aircraft cabin environment. *Aerosol Science and Technology*. 2009; 43 (4): 322-343.
54. Wei J and Li Y. Airborne spread of infectious agents in the indoor environment. *American Journal of Infection Control*. 2016; 44(9): S102-S108.
55. Jianjian Wei ,Yuguo Li (2017) Human Cough as a Two-Stage Jet and Its Role in Particle Transport Published: January 3, 2017<https://doi.org/10.1371/journal.pone.0169235>

56. Werrett, S. (2010). Fireworks: Pyrotechnic Arts and Sciences in European History. University of Chicago Press. ISBN 978-0-226-89377-8.
57. Wingerden, V. K., Hesby, I. and Eckhoff, R. (2011), Ignition of Dust Layers by Mechanical Sparks, in: Proceedings of 7th Global Congress on Process Safety, Chicago, Ill, 2011.
58. Zhang L and Li Y. Dispersion of coughed droplets in a fully-occupied high-speed rail cabin. *Building and Environment*. 2012; 47: 58-66.
59. Zhu S, Kato S and Yang J-H. Study on transport characteristics of saliva droplets produced by coughing in a calm indoor environment. *Building and Environment*. 2006; 41(12): 1691-1702.
60. Zohdi, T. I. (2007). Computation of strongly coupled multifield interaction in particle-fluid systems. *Computer Methods in Applied Mechanics and Engineering*. Volume 196, 3927-3950.
61. Zohdi, T. I. (2010) On the dynamics of charged electromagnetic particulate jets. *Archives of Computational Methods in Engineering*. Volume 17, Number 2, 109-135
62. Zohdi, T. I. (2013) Numerical simulation of charged particulate cluster-droplet impact on electrified surfaces. *Journal of Computational Physics*. 233, 509-526.
63. Zohdi, T. I. (2014) Embedded electromagnetically sensitive particle motion in functionalized fluids. *Computational Particle Mechanics*. 1: 27-45.
64. Zohdi, T. I. (2016). A note on firework blasts and qualitative parameter dependency. *Proceedings of the Royal Society*. DOI: 10.1098/rspa.2015.0720
65. Zohdi, T. I. and Cabalo, J. (2017). On the thermomechanics and footprint of fragmenting blasts. *International Journal of Engineering Science*. 118, 28-39.
66. Zohdi, T. I. (2018). Modeling the spatio-thermal fire hazard distribution of incandescent material ejecta in manufacturing. *Computational Mechanics*. <https://doi.org/10.1007/s00466-018-1617-2>
67. Zohdi, T. I., (2020) A machine-learning framework for rapid adaptive digital-twin based fire-propagation simulation in complex environments. *Computer Methods in Applied Mechanics and Engineering*. <https://doi.org/10.1016/j.cma.2020.112907>
68. Zohdi, T. I., (2020) Rapid simulation of viral decontamination efficacy with UV irradiation, *Computer Methods in Applied Mechanics and Engineering*. Volume 369 <https://www.sciencedirect.com/science/article/pii/S00466>